Journal of Radioanalytical and Nuclear Chemistry (2018) 315:557–564
https://doi.org/10.1007/s10967-017-5689-9

Detection of illicit material using neutron activation: weakness and solutions

Ali M. Al-Bahi[1] · Abdelfattah Y. Soliman[1] · Nader M. A. Mohamed[2]

Received: 30 October 2017 / Published online: 30 December 2017

Abstract
Poisoning the illicit materials by a neutron absorber leads to false detection when the detection is relied on combined thermal neutron activation and fast neutron activation to identify the elements of interest. The use of adjacent transmission thermal neutron detector for verifying the presence of neutron poisons and to trigger an alarm was investigated experimentally and using MCNP calculations. The illicit material of high hydrogen content will affect the detector response in the presence or absence of poisons.

Keywords Illicit material detection · Explosives detection · Neutron activation · Neutron poisons · Neutron transmission detection

Introduction

Detection of small amounts of modern highly explosive materials hidden in airline containers and passenger baggage is a high priority in national homeland security. Various detection methods including vapor detection, X-ray screening and neutron interrogation have been employed over the years in order to identify such explosive materials. Neutron interrogation techniques have several advantages over other methods that normally fail to identify the explosives if they are properly handled and sealed [1].

The major advantage of neutron interrogation systems is that it is hard to shield the target material from fast neutrons, which can pass through iron and lead shields with very little attenuation. X-rays and gamma rays, on the other hand, can be shielded by middle to high atomic number dense materials. Neutrons are also effective in differentiating between various types of organic materials [2]. Neutrons are not affected by electromagnetic forces, they interact only with nuclei with high specificity and can be tagged in both time and space [3].

Nuclear based explosive detection techniques have been shown to generate better results however at a higher cost and low speed [4]. These techniques include thermal neutron analysis (TNA), fast neutron analysis (FNA), pulsed fast neutron analysis (PFNA), pulsed fast thermal neutron analysis (PFTNA) and nuclear resonance absorption (NRA) of gamma rays. PFTNA technique provides a bulk analysis of the chemical present and uses 10 μs pulsing as compared to PFNA which uses 2 ns pulsing. It also has the main advantage of being portable and allows the neutrons to be moderated for the measurement of thermal neutron gamma-rays. PFTNA can provide thermal neutron information like TNA but, in addition, it also measures fast neutron interactions [5].

Statistics of the year 2010 show that approximately 10^7 pieces of luggage are checked every year at a large international airport which is translated into an inspection time of about 6 s per item [6]. Due to the diversity of the threat detection techniques, multi-level screening is becoming more popular to avoid the drawbacks of a single technique and compromise between the accuracy and the speed of the detection system [4]. A detection system composed of two units was proposed by the authors [7]. These two units are X-ray and PFTNA screening machines. The scanning starts

✉ Nader M. A. Mohamed
mnader73@yahoo.com

Ali M. Al-Bahi
abahi@kau.edu.sa

[1] Faculty of Engineering, King AbdulAziz University, Jeddah, Saudi Arabia

[2] Atomic Energy Authority, ETRR-2, Cairo, Egypt

at unit 1, which is an X-ray machine, to indicate the coordinates of the position of interest and its alarm triggers the movement of the bag to unit 2, which is PFTNA, with the proposed coordinates from unit 1. In unit 2, D–T neutron generator produces 14 MeV neutron pulse trains with 8 kHz with a 7 μs wide deuteron pulse. De-excited gamma rays from elements such as C, O and N are detected using NaI detectors and stored for further analysis. Shutting down the neutron beam for about 100 μs, allows some of the fast neutrons that remain inside the bag to be thermalized and captured by elements such as H, N, Cl and Fe. The captured gamma rays are detected by the same detectors and are recorded separately [7]. The concept design indicated that a generator of 10^{10} neutrons s^{-1} is sufficient for the detection purpose in few seconds.

One of the potential threats in the illicit material detection by PFTNA [7] is presence of shield and (or) absorber to hide the illicit material by absorbing the probing radiation. In the previous research, a thermal neutron detector is placed to detect the presence of a thermal neutron shield and produce a shield alarm. The study indicated that the flux of thermal neutrons inside the object is reduced by almost a factor of four due to coating the illicit material with cadmium sheet or mixing it with 1% boron [7]. Shield alarm is considered as a false alarm because it requires more inspection and fail to clear the presence of the threat. The aviation security standards limits the rate of false alarm, which include the shield alarm, and consequently, limits the applicability of the PFTNA. Some inventions combined two different techniques to reduce the shield alarm such as: combined nuclear quadrupole resonance and X-ray contraband detection system [8], and combined computed tomography (CT) and quadruple resonance sensors [9]. The alarm in the combined detection systems is based on analysis of data from the two techniques to contribute to decreasing the shield alarm and its contribution to the false alarm. In our design [7] a thermal detector is placed for detecting the presence of thermal neutron shield to trigger a shield alarm.

In the present research, experiments and MCNP calculations are used to investigate the importance of combining a thermal neutron transmission detector in the illicit material detection systems.

Methods

The elements detected using TNA have low thermal neutron capture cross sections and the presence of low amount of strong neutron absorber in the object will suppress the thermal neutron flux leading to false detection. A comparison between the thermal neutron capture cross sections of the elements detected by TNA and strong neutron absorption cross sections elements (poisons) is given in Table 1. One way to overcome this problem is by avoiding the detection of illicit materials using TNA and relying on the FNA only. For example, TNT material is composed of C, H, N and O with atom ratio of 7:5:3:6, respectively. FNA is used to detect C, N and O while TNA is used to detect H and N. The material can be detected by measuring the ratio between C, N and O using the FNA with eliminating the measurement of H. Another example is the cocaine hydrochloride ($C_{17}H_{22}ClNO_4$) can be detected by measuring the ratio between C, Cl, N and O using the FNA (Cl can be detected using FNA and/or TNA).

If the TNA will be considered in the detection of illicit materials, the system should detect the presence of any strong absorption cross section elements in the object. Two methods can be used to detect strong neutron absorption cross sections elements in the object. First method is based on the Prompt Gamma Neutron Activation Analysis (PGNAA). In this case the library of the illicit material detection system should be able to detect any element that has a strong absorption cross section. The main disadvantage of this method is that some strong absorption cross sections elements such as Li cannot be detected using PGNAA. The second method is based on the measurement of transmitted thermal neutrons using a thermal neutron detector. In this case, if the object contains or coated by a strong absorption cross section element, the object will act as a thermal neutron shield and the detector reading will be suppressed.

Illicit materials usually contain high atom density of hydrogen [10] which acts as a strong neutron moderator and scatterer. Therefore, the presence of an illicit object between the neutron source and the neutron transmission detector will affect the reading of the detector regardless whether the object contains neutron poisons or not. If a part of the neutron beam is thermalized before reaching the object, a significant number of the thermal neutrons will be scattered away from the transmission direction and the

Table 1 Thermal neutron capture cross sections of nuclides of interest and poisons (www.nds.iaea.org, 2017)

Nuclide	Type	Reaction	Cross section (b)
^{1}H	Component	(n, γ)	0.333
^{14}N	Component	(n, γ)	0.075
^{35}Cl	Component	(n, γ)	43.6
^{7}Li	Poison	(n, α)	940
^{10}B	Poison	(n, α)	3840
^{113}Cd	Poison	(n, γ)	60,700
^{155}Gd	Poison	(n, γ)	253,000
^{157}Gd	Poison	(n, γ)	20,000

detector reading will be decreased. When the object contains neutron poisons, more suppression in the detector reading will occur. Based on this, the neutron transmission detector will help in detecting the clean and poisoned illicit objects.

In the previous work [7], a dual detection system has been proposed. The system consists of two units. The first unit is an X-ray machine to indicate the location of interest. The second unit is a neutron based system. The location detected by the first unit is transformed to a step motor signal to identify the location of the neutron source and detectors in the second unit. The alarm from the first unit triggers the movement of the bag to the second unit while a step motor fixes the neutron source and an array of NaI detectors in the position of interest. The transmitted thermal neutron detector which will trigger the alarm system in case of the presence of neutron shield would be fixed by the motor in which the angle between the detector and source is zero as shown in Fig. 1.

Calculations

The general-purpose, continuous-energy and generalized-geometry Monte Carlo transport code, MCNPX [11] was used to simulate the detection system. The input file created by the MCNP code contains information of the problem geometry, the material description and the selection of cross-section library, the specification of the radiation source, desired tallies (answers) any variance reduction techniques used to improve the calculation efficiency. The input file is subsequently read by MCNP code and the results are printed in the output file per source particle.

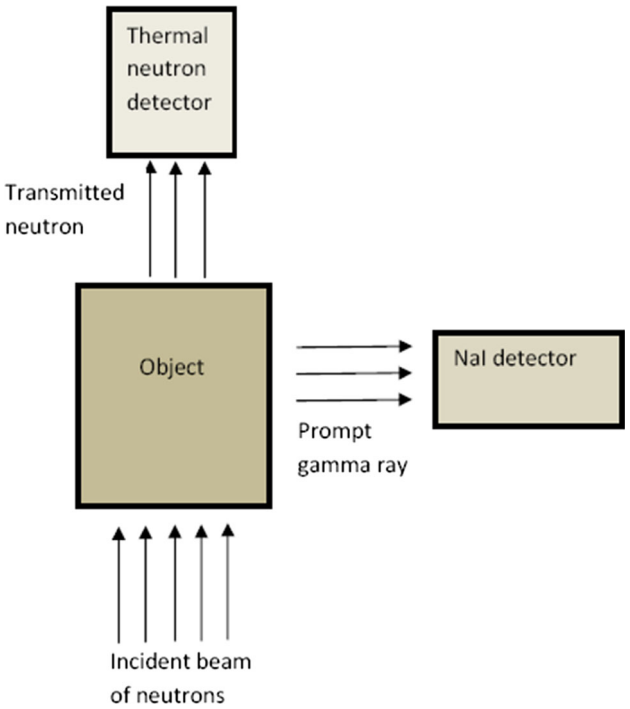

Fig. 1 Schematic diagram for the location of a thermal neutron detector in the TNA system

A $10^{D} \times 10^{H}$ cm cylindrical TNT material was simulated. The material is assumed to be composed of C, H, N and O with atom ratio of 7:5:3:6, respectively and density of 1.65 g cm^{-3}. The source is a fan-collimated of 14 MeV neutrons. Polyethylene was used in the collimations, so a spectrum of thermal, epithermal and fast neutrons will reach the object. A 3 × 3 in NaI detector was situated at 90° for the spectroscopy of gamma-rays produced in the object. The gamma-ray spectrum in the detector was calculated using F8 tally (pulse height tally) with the corresponding E tally to divide the energy range between 0.4 and 11 MeV into 10,000 channels. A BF_3 thermal neutron detector was situated at 0° to calculate the transmitted thermal neutrons. To study the effect of the presence of neutron poisons inside or around the object, four cases were studied. The first case is the reference case where the object did not contain any neutron poisons. In the second case, the object contained 0.5 wt% ^{6}Li while in the third case the object contained 1 wt% natural gadolinium. In the fourth case, it is assumed that the object was coated with 15 mg cm^{-2} (surface density) of ^{10}B.

The calculated neutron flux spectrum in the clean TNT object (case 1) is shown in Fig. 2. The effect of the neutron poisons on the neutron flux is shown in Fig. 3. Poisoning the object by 0.5 wt% ^{6}Li or coating it by 15 mg cm^{-2} ^{10}B (cases 2 and 4, respectively) reduces the thermal neutron flux to about one-sixth while poisoning it by 1 wt% natural gadolinium decreases the thermal neutron flux to about one-eighth. Since ^{6}Li has a considerable absorption cross section for the epithermal neutrons, a significant decrease in the epithermal neutron flux can be observed due to poisoning the object by 0.5wt%. ^{6}Li as shown in Fig. 3. Gadolinium is a heavy element which will replace light elements in the case of poisoning the object with it. As a result the moderation of neutrons will be affected with an increase in the number of neutrons that are partially moderated as shown in Fig. 3.

The calculated gamma ray spectrum in the NaI detector for the pure TNT object is given in Fig. 4. Figures 5 and 6 focus on the 2.22 MeV H and 10.83 N lines, respectively produced from thermal neutron activation for the four cases studied. As shown in the figures, the neutron poisons suppressed the thermal neutron activations and the detection system will give false concentration of hydrogen and nitrogen.

The response of the transmitted thermal neutron detector is almost proportional to the thermal neutron flux in the

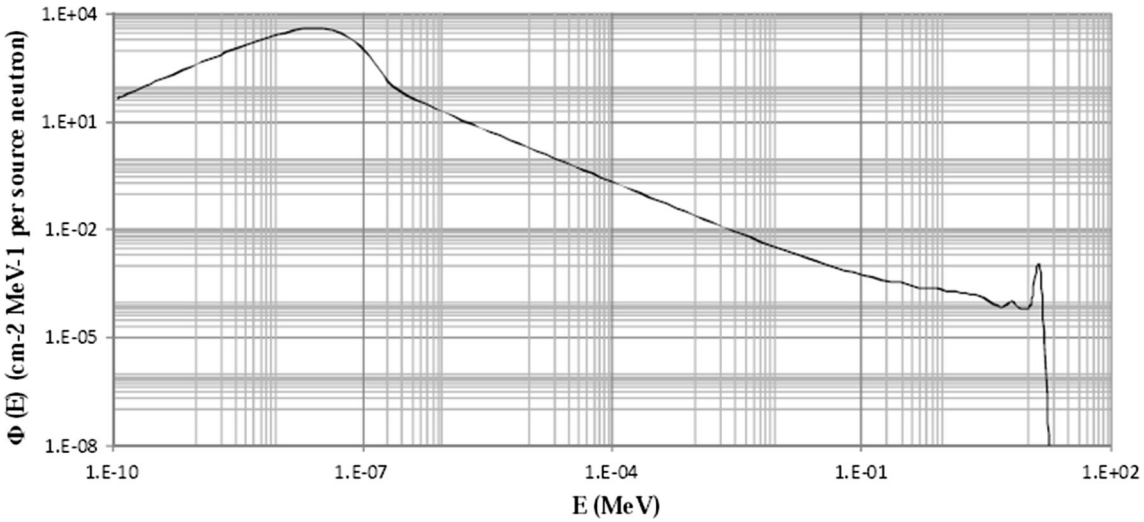

Fig. 2 Energy dependent neutron flux distributions in the TNT objects for the investigated cases

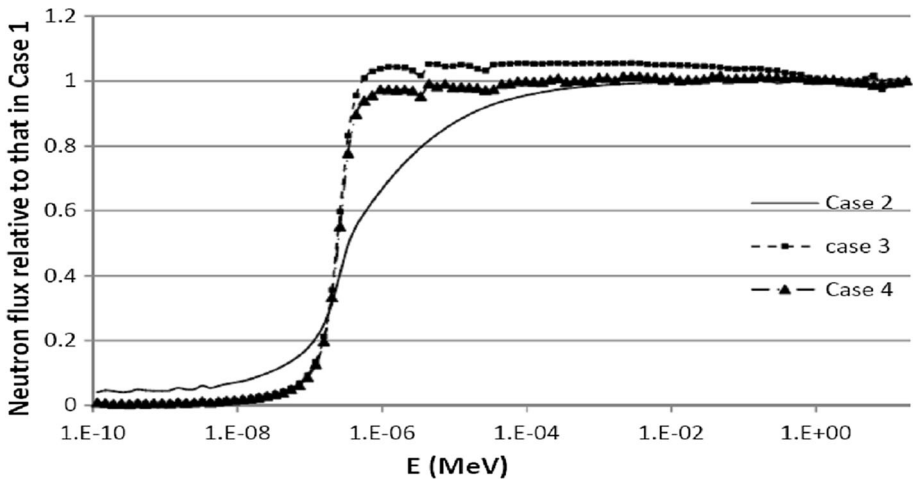

Fig. 3 Effect of neutron poisons on the neutron flux inside the TNT object

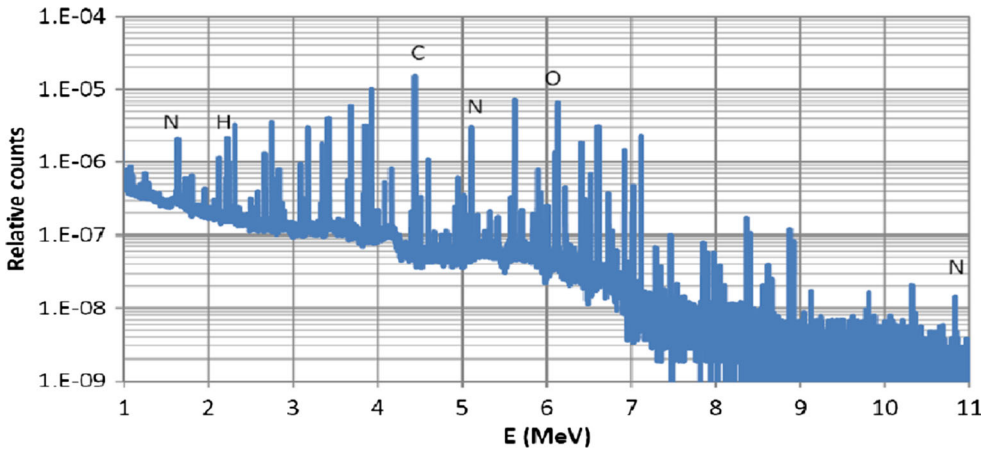

Fig. 4 Calculated gamma-ray spectrum in the NaI detector with the gamma-lines of interest

object. This in turn would detect the presence of neutron poisons in the object. The thermal neutron transmissions were calculated for a non-illicit material (nylon) and clean and 1% ^{10}B poisoned TNT objects. The non-illicit material is composed of C, H, N and O with atom ratio of 6:3:1:2, respectively and filling density of 0.15 g cm^{-3}. As given in Table 2, nylon object attenuated the thermal neutrons by 30% while the clean and poisoned TNT objects attenuated

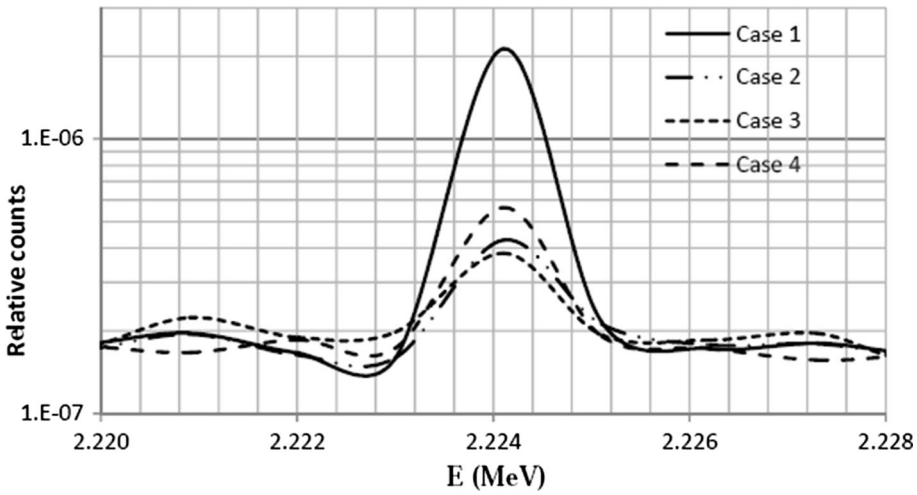

Fig. 5 Calculated 2.22 MeV H peak generated in the NaI detector for the cases studied

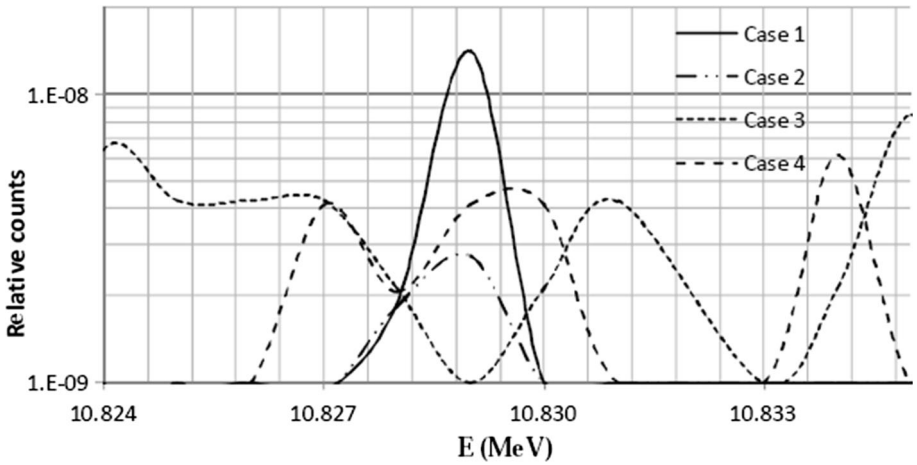

Fig. 6 Calculated 10.83 MeV N peak generated in the NaI detector for the cases studied

Table 2 Effect of illicit material on the thermal neutron transmission detector response relative to non-object response (uncertainty is within 2%)

Object	Atom ratio				Density (g cm^{-3})	Relative reading of thermal neutron transmission detector
	C	H	N	O		
Air	–	–	8	2	0.0015	1
Nylon	6	3	1	2	0.15	0.7
TNT	7	5	3	6	1.65	0.17
TNT contains 1% ^{10}B	7	5	3	6	1.65	0.02

the thermal neutrons by 83 and 98%, respectively. Based on these calculations, the transmission thermal neutron detector can help in the detection of illicit materials when they are clean or poisoned with a strong thermal neutron absorber.

Experiment design and simulation

Experimental setup

In order to validate the concept and the calculations, an experiment was conducted using two samples. The first sample was a 0.5 kg of pure ammonium chloride (NH_4Cl) and the second sample was a 0.5 kg of NH_4Cl containing 5% of a boron carbide (B_4C) powder. In this sample the ^{10}B neutron poison represents 0.8% of the sample weight.

Each sample has dimensions of 8.8 × 10 × 10.8 cm. Since the 14 MeV neutron generator was not available, a Pu–Be source with strength of 5×10^6 neutron per s was used. The source was positioned at 34 cm from the center of the object sample in a constructed shield and collimated towards the object. In order to increase the thermal neutron inside the object, a 4 cm thick 10 × 10 cm of polyethylene layer was positioned at the beam opening as shown in Fig. 7.

A 5 × 5 in NaI (Tl) detector was situated at 90° for the spectroscopy of gamma-rays produced in the object. The detector window was located at 21 cm from center of the object and the detector was shielded by 15 cm lead shield with a collimation for the gamma ray as shown in Fig. 7. The detector window was located at 21 cm from the center of the object. The detector was shielded against the thermal neutrons using around 1 mm of boron carbide to reduce the activation in the detector assembly and the associated photomultiplier tube. Pulses produced in the detector, due to the interaction of gamma-ray with detector assembly, are processed by the connected electronics including high voltage–power supply, photomultiplier tube, linear amplifier, and multi channel analyzer MCA of 1024 channels run by MAESTRO-32 software, all manufactured by ORTEC.

A $0.8^{D} \times 10^{H}$ cm ^{3}He detector was positioned at 10 cm from the object center behind the object to measure the transmitted thermal neutrons (Fig. 7). The detector was shielded using 0.5 mm cadmium sheet while a window with length of 2.5 cm was opened for the measurement. The produced pulses in the detector are fed to a preamplifier, then to an ORTEC 572A amplifier and then to a counter which integrates pulses produced from the interactions of the thermal neutrons with ^{3}He gas at reaction Q-value of 0.764 MeV.

MCNP simulations

The experiment was simulated using the MCNPX code to calculate the pulse height spectrum in the detector and the thermal neutron transmission rate. The simulated model is shown in Fig. 7. The source energies were simulated by dividing the neutron spectrum into 13 groups. The pulse height spectrum was calculated as described above ("Calculations"). The ^{3}He detector pulses was calculated using the F4 tallies (flux average in a cell) with the corresponding multiplier card, FM. This card is used to calculate the interaction rate in the detector:

$$R = N \int \sigma_{(n,p)}(E)\phi(E)\mathrm{d}E, \quad (1)$$

where N is the total number of ^{3}He atoms, $\sigma_{(n,p)}$ is neutron cross section for the reaction: ${}^3_2\mathrm{He}(n,p){}^3_1\mathrm{H}$ and $\phi(E)$ is the energy-dependent flux. The background in the pulse height spectrum of gamma rays was eliminated by setting zero photon importance for all the cells except the object and the NaI detector. Also, in the calculation of the ^{3}He detector response, all the cells that is not in the direction of the neutron beam have zero neutron importance to eliminate the background due to the neutron scattered by these cells.

Results and discussions

The measurement for the background and the two samples lasted for 3600 s. The measurements were focused on

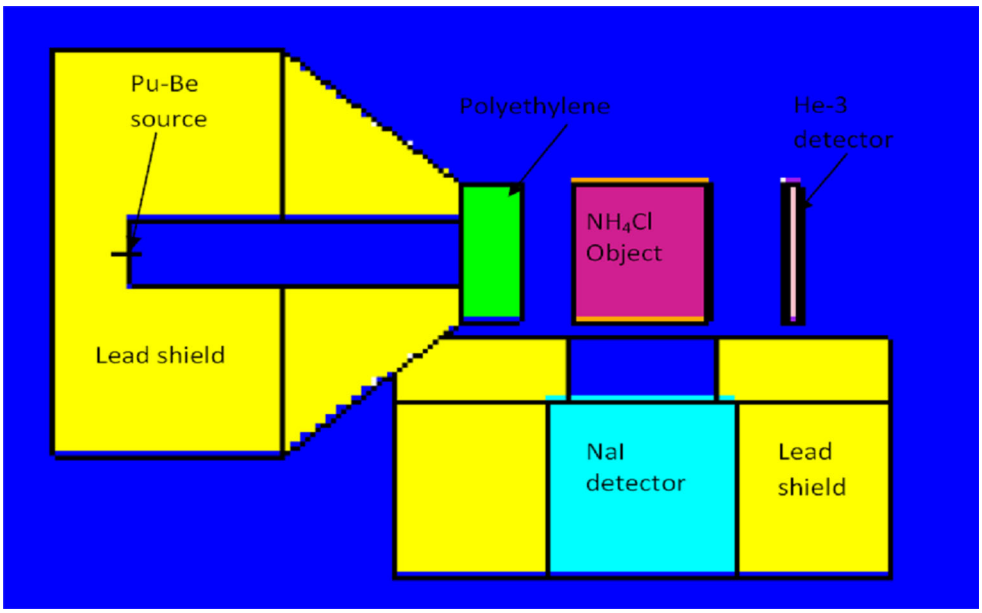

Fig. 7 MCNP model of the experiment

Table 3 Measured and calculated count rates of the NaI detector for the hydrogen 2.22 MeV gamma-ray line

Sample no.	Description	H Count rate, C_{net} (s^{-1}) (standard deviation, σ_C, %)		
		Measured	Calculated	Deviation (%)
1	0.5 kg NH_3Cl	0.55 (20)	0.604 (3)	9.7
2	0.5 kg of NH_3Cl contains 5% B_4C	$< D_L$	0.21 (4)	–

Table 4 Measured and calculated count rates of ^{3}He detector

Case	Description	Count rate (s^{-1}) (standard deviation, %)		
		Measured	Calculated	Deviation (%)
1	Without the object	3.27 (4)	3.22 (3)	− 2
2	0.5 kg of pure NH_3Cl between the source and the object	0.502 (10)	0.462 (3)	− 8
3	0.5 kg of NH_3Cl contains 5% B_4C between the source and the object	$< D_L$	0.172 (3)	–

hydrogen line. The count rate, C_{net} for each sample was calculated by subtracting the background from the net peak area:

$$C_{net} = \frac{N_S - N_{BG}}{t}, \quad (2)$$

where N_S and N_{BG} are the net peak areas for the sample and for the background, respectively and t is the counting time. The standard deviation associated with the C_{net}, σ_C is:

$$\sigma_C = \sqrt{\frac{\sigma_{net}^2 + \sigma_{BG}^2}{t}}, \quad (3)$$

where σ_{net} and σ_{BG} are the standard deviations in N_S and N_{BG}, respectively. The detection limit, D_L can be estimated to be three times of the standard deviation, σ_C [12]:

$$D_L = 3\sigma_C \quad (4)$$

Based on this, hydrogen will be detectable if:

$$C_{net} > 3\sigma_C \quad (5)$$

The presence of the polyethylene layer at the beam opening increased the background and therefore the uncertainty in the counting. The measured count rate for the pure NH_4Cl object, C_{net} was 0.55 s^{-1} with a standard deviation, σ_C of 20%. Poisoning the object with 0.8% of ^{10}B made the count rate under the detection limit ($\sigma_C > 33\%$). MCNP code prints the results per source particle, therefore the results were multiplied by the source strength i.e. 5×10^6 s^{-1}. The calculated count rate for the pure NH_4Cl object was 0.604 s^{-1} while it was 0.21 s^{-1} for the poisoned object as given in Table 3. The standard deviation in the calculations were around 4%. As given in the table the deviations between the calculations and the measurements is around 10%.

In the measurement of the neutron transmission using the ^{3}He detector, the background was measured by shielding the front side of the polyethylene layer by 1 mm of boron carbide. Then, the transmission with and without NH_4Cl objects were counted for 300 s. Five readings for each measurement were recorded and the average values and the standard deviations were calculated after subtracting the background as given in Table 4. The MCNP calculation results are given in Table 4, as well. The presence of the object between the source and the detector reduces the count rates significantly because of the scattering of the object to the neutrons removing them from the transmission direction. Also, poisoning the object with 0.8% of ^{10}B made the count rate under the detection limit of the measurements. The deviations between the calculations and the measurements is 2% for the case where there is no object between the source and the detector. In the case of the presence of the object, the count rate became low and the uncertainty is increased making the deviation between the measurements and calculations around 8% as given in Table 4.

Conclusion

Use of thermal neutron activation in the detection of illicit materials is unreliable since a small amount of thermal neutron absorber makes the neutron self-shielding very high leading to false detection. One way to overcome this weakness is by avoiding the use of thermal neutron activation in the detection and relying on fast neutron activation only, however this will limit the number of elements to be identified. The second solution is by detecting the presence of neutron poisons using a transmitted thermal neutron detector which will trigger the alarm system in case of the presence of neutron shield. Moreover, illicit materials usually contain high atom density of hydrogen and therefore the detector can help in the detection of illicit

materials when they are clean or poisoned, as a second screening method.

Acknowledgements This project was supported by the NSTIP Strategic Technologies Program in the Kingdom of Saudi Arabia, Project No. 10-MAT 1267-03. The authors also acknowledge with thanks the Science and Technology Unit at King Abdulaziz University for their technical support.

References

1. Whetstone ZD, Kearfott KJ (2014) A review of conventional explosives detection using active neutron interrogation. J Radioanal Nucl Chem 301:629–639
2. Liu Y, Sowerby BD, Tickner JR (2008) Comparison of neutron and high-energy X-ray dual-beam radiography for air cargo inspection. Appl Radiat Isotopes 66(4):463–473
3. Buffler A (2004) Contraband detection with fast neutrons. Radiat Phys Chem 71:853–861
4. Singh S, Singh M (2003) Explosives detection systems (EDS) for aviation security: a review. PANN Research, University of Exeter, Exeter
5. Womble PC, Vourvopoulos G, Novikov I, Paschal J (2001) PELAN 2001: current status of the PELAN explosives detection system. In: Proceedings Volume 4507, Hard X-Ray and Gamma-Ray Detector Physics III. https://doi.org/10.1117/12.450762
6. Liu X, Gale A (2011) Air passengers' luggage screening. What is the difference between naive people and airport screeners? In: 9th international conference engineering psychology and cognitive ergonomics, pp 424–431
7. Al-Bahi AM, Soliman AYA, Hassan MHM, Mohamed NMA (2014) Concept design of an illicit material detection system. J Radioanal Nucl Chem 299:351–356
8. Laubacher DB (2007) Metal shield alarm in a nuclear quadrupole resonance/X-ray contraband detection system. US Patent No: US 2007/0229069 A1
9. Skatter S, Rayner TJ, Petrov TR, Clark KA, Chemouni S, Mann K, Surrey C (2004) Explosives detection system using computed tomography (Ct) and quadrupole resonance (Qr) sensors. US Patent No: US 2004/0252807 A1
10. Bruschini C (2001) Commercial systems for the direct detection of explosives for explosive ordnance disposal tasks. Subsurf Sens Technol Appl 2:299–336
11. Pelowitz DB (2011) MCNPX user's manual, version 2.7.0. Los Alamos National Laboratory, Los Alamos
12. Thomsen V, Schatzlein D, Mercuro D (2017) Limits of detection in spectroscopy. http://chekhter.de/wp-content/uploads/2012/04/LODs.pdf